APPLIED AND ENVIRONMENTAL MICROBIOLOGY, Dec. 1994, p. 4339–4344
0099-2240/94/$04.00+0

Vol. 60, No. 12

Direct Measurement of Chlorine Penetration into Biofilms during Disinfection

DIRK DE BEER,[1]† ROHINI SRINIVASAN,[2]‡ AND PHILIP S. STEWART[2]*

Center for Biofilm Engineering[1] and Department of Chemical Engineering,[2] Montana State University, Bozeman, Montana 59717

Received 20 June 1994/Accepted 29 September 1994

Transient chlorine concentration profiles were measured in biofilms during disinfection by use of a microelectrode developed for this investigation. The electrode had a tip diameter of ca. 10 μm and was sensitive to chlorine in the micromolar range. The biofilms contained *Pseudomonas aeruginosa* and *Klebsiella pneumoniae*. Chlorine concentrations measured in biofilms were typically only 20% or less of the concentration in the bulk liquid. Complete equilibration with the bulk liquid did not occur during the incubation time of 1 to 2 h. The penetration depth of chlorine into the biofilm and rate of penetration varied depending on the measurement location, reflecting heterogeneity in the distribution of biomass and in local hydrodynamics. The shape of the chlorine profiles, the long equilibration times, and the dependence on the bulk chlorine concentration showed that the penetration was a function of simultaneous reaction and diffusion of chlorine in the biofilm matrix. Frozen cross sections of biofilms, stained with a redox dye and a DNA stain, showed that the area of chlorine penetration overlapped with nonrespiring zones near the biofilm-bulk fluid interface. These data indicate that the limited penetration of chlorine into the biofilm matrix is likely to be an important factor influencing the reduced efficacy of this biocide against biofilms as compared with its action against planktonic cells.

Biofouling is the detrimental development of biofilms in engineered systems, such as industrial process equipment, drinking water distribution systems, and ship hulls. Biofilms can decrease heat transfer in heat exchangers, increase the pressure drop in pipelines (5, 14), and enhance corrosion (10, 14) and may be a source of bacterial contamination of drinking water (4). Biofilms are a nuisance in these systems, and control of their development may be necessary to maintain process efficiency and safety. Biofilm control is often performed with biocides, of which the most commonly used is chlorine, a strong oxidizing agent and disinfectant. Biocides are much less effective against biofilms than suspended cells (6, 11–13, 15). Cells in biofilms are protected from biocide action and are killed only at biocide concentrations orders of magnitude higher than necessary to kill suspended cells. It has been speculated that the lower sensitivity of biofilm cells to biocides is due to differences in the physiological state associated with lower growth rate (3). Alternatively, biocides may not reach the cells as a result of diffusional resistance of the biofilm matrix (7) or neutralization of the biocide inside the matrix (15, 18).

The objective of this study was to determine biocide penetration into a microbial biofilm during biocide treatment. Direct concentration measurements in biofilms can be achieved with high spatial resolution by use of microelectrodes, as shown for oxygen (9, 17), pH (9, 17), sulfide (17), nitrate (9), and ammonium (9). These needle-shaped sensors have a tip diameter of 1 to 10 μm, which prevents disruption of the biofilms during measurements. We developed a microsensor for chlorine and compared measurements of biocide penetration with previously developed methods to assess biocide action in biofilms.

* Corresponding author. Phone: (406) 994-2890. Fax: (406) 994-6098.

† Present address: Microbial Ecology Laboratory, University of Ghent, 9000 Ghent, Belgium.

‡ Present address: Orange County Water District, Fountain Valley, CA 92728.

MATERIALS AND METHODS

Biofilm growth. Biofilms were developed in a continuous-flow annular reactor that incorporated 12 removable stainless-steel slides to permit sampling of the biofilms growing on them. Binary population biofilms of *Pseudomonas aeruginosa* and *Klebsiella pneumoniae* were developed by inoculating the reactor with frozen stock cultures, incubating the cultures in batch mode for 24 h, and then initiating flows to sustain continuous culture as described previously (6). Experiments were performed with 1-week-old biofilms having a maximal thickness of 150 to 200 μm.

Chlorine microelectrode preparation. The microelectrode was patterned after an oxygen microelectrode (17), modified to obtain a miniaturized version of a chlorine macroelectrode (2). The cathode was made from 100-μm-diameter platinum wire, of 99.99% purity, that was tapered to a fine tip (less than 1 μm) on one end and sealed in a glass capillary as described previously (17). Before applying the glass coating, the wire was rinsed in distilled water and acetone and dried with a hot-air gun. After the platinum tip was exposed by grinding (17), the glass was resealed by reheating the tip for ca. 2 s with a heating coil. Subsequently, the platinum in the tip was recessed 1 to 2 μm in a fresh 2 M KCN solution while applying 2.5 V of alternating current. The tip was then rinsed in distilled water and acetone, dried with a hot-air gun, and dipped in a solution of 10% (wt/vol) cellulose acetate in acetone for 30 s. After applying the cellulose acetate coating, the acetone was allowed to evaporate for 1 h at room temperature. The tip diameters of the resulting microelectrodes were 5 to 10 μm. Stirring effects were determined by measuring the microelectrode signal in a chlorine solution of 10 to 20 μM that was either stirred or stagnant. The velocity of the stirred liquid was at least 30 cm/s. If the signal difference was more than 5%, the electrodes were washed with distilled water, dried, and recoated. Microelec-

trodes were rinsed with distilled water after use and stored on the shelf.

Microelectrode measurements. During calibration and concentration measurements, the potential of the microelectrode was maintained at +0.2 V relative to a double-junction Ag-AgCl reference electrode by using a battery-operated power source. Current was measured with a Keithley 617 multimeter. Calibration was performed in a stirred beaker. The sensitivity of the electrode to interference by 10 mM NaCl, 10 mM $CaCl_2$, 10 mM sodium phosphate (pH 7.0), 5.5 mM glucose, 0.1% (wt/vol) sodium alginate, or 0.1% (wt/vol) bovine serum albumin (BSA) was tested in sterile growth medium with 0.03 mM chlorine. The pH sensitivity was tested in a buffer containing 10 mM sodium phosphate, 10 mM boric acid, and 10 mM sodium carbonate, supplied with 0.14 mM chlorine; the pH was varied by addition of 1.5 N HCl or 2 M NaOH. For measurement of microprofiles in biofilms, the electrode was mounted on a micromanipulator with a stepper motor, allowing 1-μm positioning accuracy. A slide covered with biofilm was placed in a polycarbonate flow cell (2.5 by 21 by 2 cm). To reduce noise, the flow cell, micromanipulator, and the battery-operated power source were placed in a Faraday cage. A medium identical to growth medium with the exception of the glucose concentration (5.5×10^{-4} mM) was introduced in the flow cell by gravity feed at a rate of 2 ml/s, resulting in an average liquid velocity of 1 cm/s. Medium was removed from the flow cell by vacuum suction; the fluid level in the flow cell was maintained at 1 cm above the slide. Positioning of the microelectrode at the biofilm surface was performed with the aid of a binocular microscope.

Measurements were started by introducing chlorine in the medium by adding a 40-times-concentrated solution to the flow cell influent. The pump used to deliver chlorine was separated electrically from the feed solution by a drip chamber. Microprofiles were measured at regular time intervals during 1 to 2 h. Each profile could be recorded in approximately 2.5 min. During the experiments, the chlorine concentration in the bulk was measured regularly with a colorimetric test kit (model CN-66; Hach Co.). The accuracy of this assay was estimated to be ±15% by comparison with the *N,N*-diethyl-*p*-phenylenediamine (DPD) colorimetric method (1).

Plate counting. After the microelectrode experiments were done, half of the slide covered with biofilm was used for determination of the decrease in viable cell number by plate counts. Slides were removed from the flow cell, and the biofilms were scraped into 100 ml of phosphate-buffered saline, homogenized, and spread plated on R2A agar medium in triplicate (11).

Microscopic examination of cross-sectioned biofilms. After the microelectrode experiments were done, the region where the microprofiles were recorded was subjected to microscopic examination. An area of ca. 0.5 cm^2 was incubated for 2 h with 5-cyano-2,3-ditolyl tetrazolium chloride (CTC; Polyscience) to stain actively respiring cells (20) and counterstained for 0.5 h with 4′,6-diamino-2-phenylindole (DAPI; Sigma) to stain both live and dead cells. The biofilm was cryoembedded and cryosectioned as described previously (19). The cross sections were examined with an Olympus BH-2 microscope with a DPlanApo 20 UV objective. The excitation wavelength used for DAPI was 360 nm, and for CTC, it was 545 nm.

RESULTS

The chlorine microelectrodes used in this investigation showed a linear response towards chlorine up to a concentration of 7.5 mM, the highest concentration tested. As shown in Fig. 1A, the electrode displayed good sensitivity (1 pA/μM) at low concentrations in the range relevant for biofilm experiments. This sensitivity is comparable to that reported for oxygen microelectrodes and is readily measured by commercial ammeters. The response time to attain 90% of the final signal was less than 1 s, and stirring sensitivity was negligible. The response in a 0.03 mM chlorine solution was not influenced (<7% change) by 10 mM NaCl, 10 mM $CaCl_2$, 10 mM sodium phosphate (pH 7.0), or 5.5 mM glucose. The addition of 1 g of Na alginate per liter resulted in a slow decrease of the signal (50% in 10 min), while the addition of 1 g of BSA per liter caused an instantaneous (<3-s) reduction of the signal to the background level. The signal decrease was accompanied by a decrease of the chlorine concentration in the medium as measured by the Hach test kit. The signal was restored to its original level upon replacement of the solution with fresh medium containing 0.03 mM chlorine. Thus, the signal decrease was due to chlorine consumption by alginate and BSA in the medium and not to a change in electrode characteristics. The electrode sensitivity to monochloramine was ca. 20% of that for chlorine. The signal decreased with increasing pH (Fig. 1B), and the pH effect was completely reversible. This suggests that the electrode responds to HClO rather than to ClO^-. However, the relation between the signal and the HClO

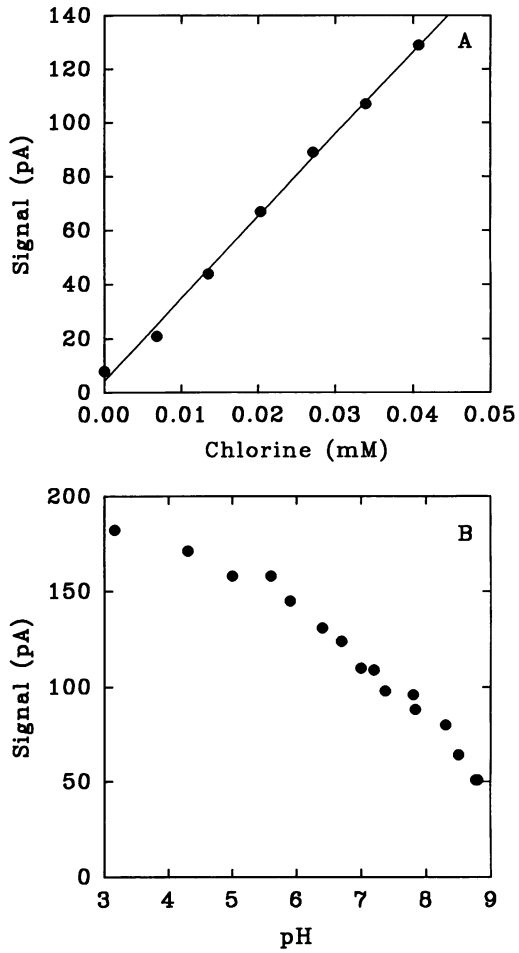

FIG. 1. (A) Calibration line of a chlorine microelectrode in sterile growth medium without glucose; (B) pH influence on the signal of a chlorine microelectrode.

concentration was not linear (data not shown). The electrode could be used for several months without deterioration of the response; in our experiments, the lifetime of the electrodes was always determined by breakage.

Biofilm was clearly visible on the stainless-steel slides with the binocular microscope. The slides were not homogeneously covered by biofilm but rather were covered by biofilm in 2-cm-wide patches positioned at equal distances along the length of the slide. These patches consisted of 150- to 200-μm-thick and 200- to 300-μm-wide cell clusters separated by voids, as observed previously (8). Chlorine profiles were measured in these cell clusters. Control experiments on sterile stainless-steel slides showed an absence of chlorine gradients. A measurement in a biofilm incubated without chlorine showed no influence of the biofilm on the background signal.

All chlorine concentration profiles recorded immediately (within 3 min) after chlorine addition showed profound concentration gradients over distances of a few hundred micrometers or less. The profiles had a sigmoidal shape, and the inflection point was usually at the biofilm surface as estimated visually. After the initial stage, however, the development of chlorine microprofiles showed a large variation. No evidence of disruption of the biofilm by repeated probing was seen.

A time series of microprofiles recorded at a bulk concentration of 0.062 mM chlorine showed a gradual penetration of chlorine in the biofilm (Fig. 2A). Even after 105 min, however, chlorine remained depleted in the biofilm interior. The inflection point of the concentration profile moved in the direction of the substratum; it travelled ca. 70 μm in 105 min. Duplication of this experiment showed similar results (Fig. 2B). In one experiment, microprofiles were recorded simultaneously at two different locations, 2.3 mm apart, on the same slide. The electrode was shuttled between the two locations by means of a motorized stage with micrometer precision. Microprofiles, recorded in the middle (position A) and on the upstream edge of a biofilm patch (position B), showed large differences in chlorine penetration rates (data not shown). At position A, the microprofiles were unchanged during a 1-h experiment, while at position B, a gradual penetration of chlorine took place. Usually, the chlorine penetrated after 1 h of treatment to a depth of 80 to 120 μm into the biofilm. In one experiment, complete penetration within 15 min was observed.

At very high chlorine bulk concentrations (0.28 to 0.42 mM), complete penetration of the biofilm was always found, although with varying rates. Penetration to 150-μm depth required 30 min in one spot (Fig. 3A), but in another location, 3 min was required (Fig. 3B). Especially in the experiments with high chlorine concentrations, the chlorine bulk concentration consistently increased during the measurements. This is probably because the chlorine demand of the system decreased by reaction of the available reducing equivalents with chlorine.

The variation in penetration rates in comparable biofilms under comparable conditions is clearly demonstrated in Fig. 4. The penetration depth (defined as the distance from the cell cluster surface to the location where the chlorine concentration is 10% of the bulk concentration) varied strongly at both low and high concentrations.

The microprofiles showed the presence of a significant mass boundary layer, with a thickness of ca. 100 to 400 μm. The chlorine concentration gradually decreased in the boundary layer from the level in the bulk to that at the biofilm surface. The biofilm surface concentration was typically 20 to 30% of the bulk concentration.

Measurements performed with a 0.062 mM chlorine bulk concentration showed no influence of the presence of 20 mM glucose on the chlorine penetration.

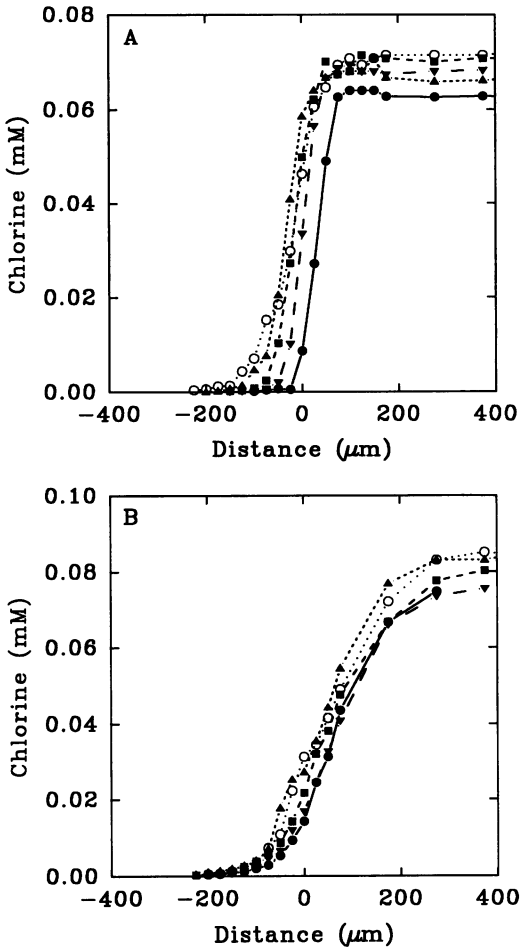

FIG. 2. Transient chlorine profiles in biofilms at a bulk chlorine concentration of ca. 0.07 mM. The chlorine profiles were recorded 3 (●), 20 (▼), 30 (■), 50 (▲), and 105 (○) min after the start of the chlorine dosing (A) or 3 (●), 25 (▼), 45 (■), 60 (▲), and 75 (○) min after the start of chlorine dosing (B). Zero on the *x* axis corresponds to the surface of the cell cluster as estimated visually at the start of the experiment.

Microscopic images of cryoembedded cross sections of biofilms stained with both CTC and DAPI are shown in Fig. 5. Without biocide treatment, the whole biofilm was stained with both CTC and DAPI, indicating the presence of respiratorily active cells throughout the biofilm. At biocide concentrations of approximately 0.07 mM, CTC staining was confined to the lower part of the cell clusters; the upper 100 μm stained only with DAPI. At high chlorine bulk concentrations (0.28 to 0.42 mM), no CTC staining was observed, but the biofilm could be stained with DAPI.

Viable counts, obtained from slides immersed for 60 min in the flow cell, were 8.69×10^{12} CFU/m^2 without chlorine addition, 3.27×10^{11} CFU/m^2 with 0.43 mM chlorine, 5.26×10^{10} CFU/m^2 with 0.085 mM chlorine, and 1.8×10^{11} CFU/m^2 with 0.28 to 0.42 mM chlorine.

DISCUSSION

A selective and sensitive chlorine microelectrode was successfully prepared. Selectivity of microelectrodes is achieved by choosing the right potential and coating. Coating of microelec-

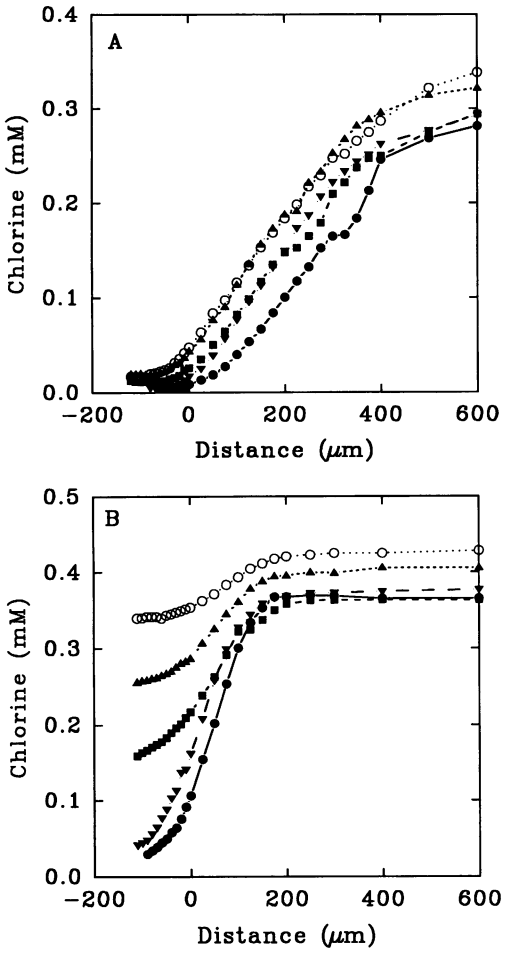

FIG. 3. Transient profiles measured at high chlorine concentrations (0.28 to 0.42 mM). The chlorine profiles were recorded 3 (●), 15 (▼), 30 (■), 45 (▲), and 60 (○) min after the start of the chlorine dosing. Zero on the x axis corresponds to the surface of the cell cluster as estimated visually at the start of the experiment. Although the conditions were similar, differences between the results shown in panels A and B are very large.

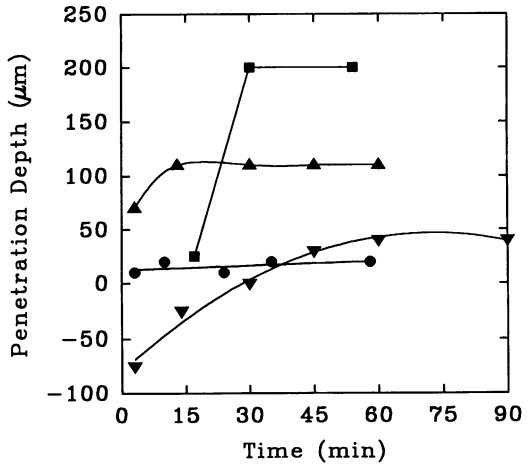

FIG. 4. Penetration depth of chlorine at 0.062 (●), 0.07 (■), 0.28 (▲), and 0.36 (▼) mM chlorine concentrations in the bulk liquid. The penetration depth is expressed as the distance from the biofilm surface to the point where the local chlorine concentration is 10% of the bulk concentration. The variation in penetration rate is large at both high and low chlorine concentrations in the bulk liquid.

trodes is also necessary to protect the catalytic surface from adhering cells and proteins as well as to reduce the stirring sensitivity by imposing a diffusive resistance in the microelectrode larger than the external diffusive resistance. DePeX, the coating commonly used for O_2 microelectrodes (17), is not permeable for chlorine. Cellulose acetate is hydrophilic and permeable for both O_2 and chlorine. At −0.7 V, both O_2 and chlorine are reduced; O_2 selectivity is then achieved by the coating. At +0.2 V, oxygen is not reduced, but chlorine still reacts at the electrode. Also, other strongly oxidized compounds may be reduced, such as monochloramine and Br_2. Monochloramine, a potential interfering species, is formed upon oxidation of ammonium by chlorine. However, since no ammonium is present in the medium, the source for monochloramine formation is limited to biomass. Moreover, the sensitivity of the electrodes for monochloramine is much lower than for chlorine; therefore, its influence on the measurements is expected to be minimal.

pH profiles in the biofilm will influence the chlorine measurements because of the pH sensitivity of the microelectrode. Possible reactions that may induce a pH change are the microbial conversion of glucose and the oxidation of biomass by chlorine. Both reactions will decrease the pH and thus lead to an overestimation of the chlorine concentrations in the biofilm. Consequently, the pH sensitivity does not undermine the conclusion that the chlorine concentrations in biofilms are low. The magnitude of the pH decrease due to chlorine reduction can be estimated from the produced acid concentration in the biofilm and the alkalinity balance. The maximal possible acid concentration difference between the bulk and the point of chlorine exhaustion inside the biofilm is calculated from the stoichiometry and diffusivity of the mobile reactants (chlorine and protons) by using the formula $P = D_{chl}YS_0/D_p$, where P is the maximal acid concentration, Y is the acid yield on chlorine (moles per mole), S_0 is the chlorine concentration in the bulk, D_{chl} is the chlorine diffusion coefficient (1.44×10^{-9} m^2/s [16]), and D_p is the diffusion coefficient of the acid product. The diffusion coefficient of the product (protons) was assumed, most conservatively, to be equal to that of hydrogen phosphate. From the alkalinity balance, it was estimated that the maximal pH shift in the biofilm was 0.3 pH unit at a chlorine bulk concentration of 0.42 mM, 0.2 unit at a bulk chlorine concentration of 0.28 mM, and 0.05 unit at a chlorine concentration of 0.07 mM. In Fig. 1B, it can be seen that the signal increase around pH 7.0 is ca. 30% per pH unit. This means that the overestimation of the chlorine concentration in the biofilm, due to the pH sensitivity of the microelectrode, was less than 6% for the highest applied chlorine concentrations, while for most measurements, the overestimation was less than 2%.

The transient chlorine microprofiles show a slow chlorine penetration into the biofilm, with a rate depending on the chlorine bulk concentration. The sigmoidal shapes of the profiles are characteristic for a substrate that is diffusing into a matrix where it is consumed. At the inflection point, no significant discontinuity is present, indicating that the diffusivity inside the biofilm is close to that in the bulk phase. If chlorine were diffusing only and not reacting within the biofilm, it would eventually fully penetrate the biofilm at the bulk concentration. The time necessary to reach a chlorine

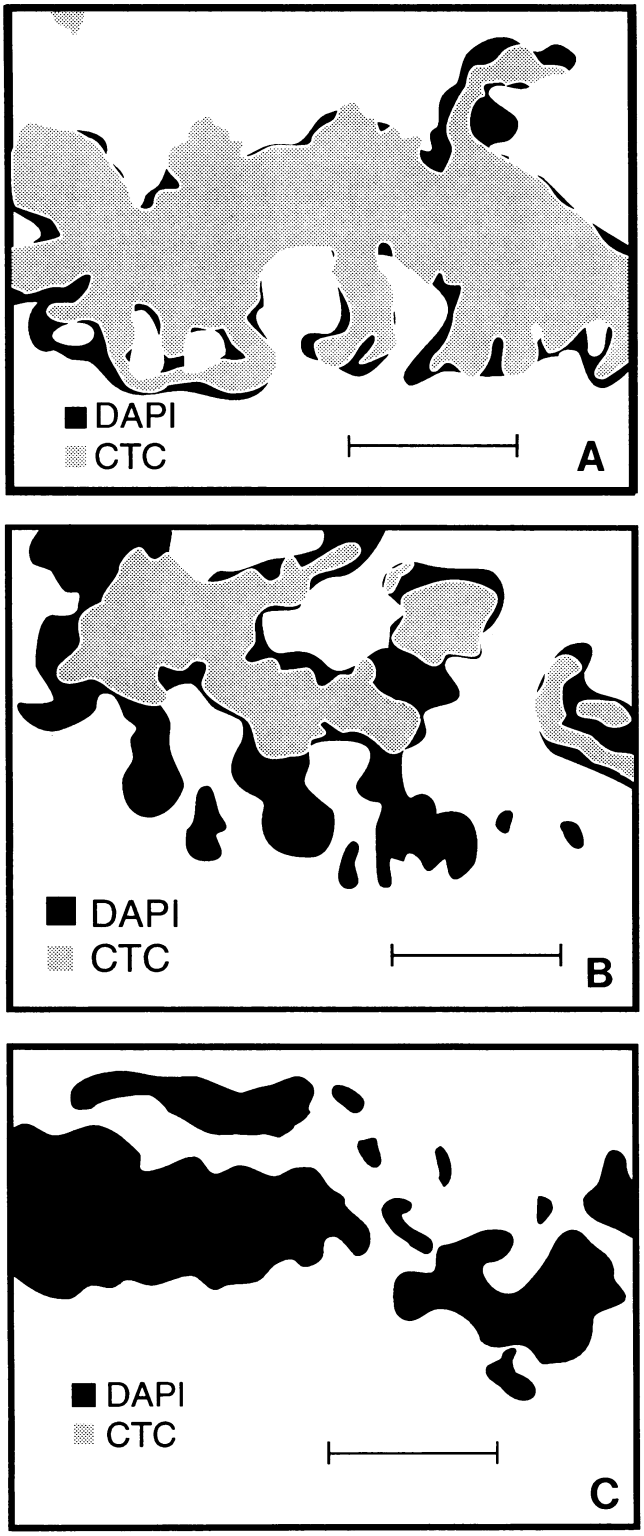

FIG. 5. Microscopic images of cross sections of cryoembedded biofilms stained with CTC and DAPI. The shaded areas indicate where CTC is excited in the images. The whole biofilm, including the dead cells, is stained with DAPI. (A) No treatment; (B) treatment with 0.07 mM chlorine for 1 h; (C) treatment with 0.28 mM chlorine for 1 h. The bulk fluid was at the bottom and the substratum was at the top in each panel. The scale bar equals 100 μm.

concentration at the substratum of 99% of the bulk concentration can be estimated from the Fourier number [$Fo = (D_{chl} \cdot t)/r^2$, where r is total diffusive pathlength, t is time, and Fo equals 2 (16)]. Since the biofilm was 150 to 200 μm thick and the diffusive boundary layer, during the experiments, was ca. 100 μm, the total diffusive pathlength was 250 to 300 μm; assuming D_{chl} is 1.44×10^{-9} m^2/s (16), it can be calculated that equilibrium will be reached within 1.5 to 2 min. The actual equilibration time appeared to be concentration dependent and, even at the highest concentration tested, exceeded 60 min. Consequently, the limited penetration is not due simply to transient diffusion but is caused by neutralization of the chlorine in the biofilm matrix.

The two possible substrates for chlorine reduction are glucose from the bulk liquid and biofilm material. The chlorine fluxes, calculated from the microprofiles by using Fick's first law, ranged from 2.2×10^{-7} to 2.9×10^{-6} mol/m^2-s. The maximum glucose flux can be estimated by assuming the biofilm surface concentration is zero and the boundary layer is the same as that for chlorine (100 to 400 μm). By using a diffusion coefficient of 6.7×10^{-9} m^2-s, the calculation results in a maximum possible glucose flux of 4×10^{-9} mol/m^2-s, 2 orders of magnitude below the lowest measured chlorine flux. Moreover, a 200-fold increase in the glucose concentration did not reduce the chlorine penetration. Consequently, the biofilm matrix material itself, consisting of cells and extracellular polymeric substances, is the substrate for chlorine neutralization.

Comparison of the cross sections and chlorine microprofiles leads to the conclusion that decreased action of chlorine against biofilms is due to limited penetration stemming from a reaction-diffusion interaction. The microprofiles show that, after exposure to 2.5 ppm of chlorine for 1 h, only the upper 100 μm of the cell clusters is penetrated by chlorine. This correlates reasonably well with the microscopic images showing that the top half of the cell clusters have lost their respiratory activity. Exposure to very high chlorine concentrations leads to complete penetration of biocide and also stops the respiratory activity in the whole biofilm.

The finding that chlorine is reduced in the biofilm matrix allows calculation of chlorine profiles in the biofilm by use of a reaction-diffusion model such as those conventionally used for modeling of substrate and product profiles. It should be noted that a one-dimensional model, calculating profiles in the direction perpendicular to the substratum only, may underestimate the chlorine transport rate into the biofilm. The biofilms contained voids that will act as transport channels at high liquid velocity (8). Consequently, lateral chlorine gradients will also develop, leading to increased exchange with the bulk liquid.

The microprofiles show the presence of a significant mass boundary layer, which is the zone in the near vicinity of the biofilm where the concentration gradually changes from the bulk level to the concentration at the biofilm surface. The chlorine concentration at the biofilm surface was 20 to 30% of the bulk concentration; thus, external mass transport resistance is significant under the experimental conditions. The mass boundary layer thickness is negatively correlated to the liquid velocity; consequently, the efficacy of biocide treatment can be strongly improved by imposing higher liquid velocities. Indeed, experiments performed in an annular reactor, with liquid velocities of ca. 1 m/s, showed much higher chlorine efficacy.

The large variability in penetration rates under comparable conditions suggests the presence of local differences within biofilms with respect to resistance to chlorine efficacy. Those

highly resistant spots may have a higher reducing capacity than the spots that are more rapidly penetrated. This could be caused by a higher cell density, subpopulations with higher reducing capacity per cell (e.g., reserve material), a higher density of extracellular polymeric substances, or extracellular polymeric substances with higher reducing potential. The phenomenon of rapid regrowth after biocide treatment may originate from such highly resistant spots. Alternatively, local differences in hydrodynamics, resulting in different chlorine transfer rates from the bulk liquid, may explain part of the differences. Comparison of Fig. 3A and B shows that increased resistance may be caused by a locally thicker boundary layer.

The plate counts show that biocide treatment results in a reduction in viable counts of 1 to 2 orders of magnitude. No clear relation with the chlorine concentration was apparent. The viable count reduction was lower at the highest chlorine concentration than at the intermediate concentration. This may be due to variability in the total cell number and cell distribution on different sample slides. It should be noted that the biofilm areas used for plate counting were smaller than those in previous studies (6, 11).

Their fragility and noise sensitivity makes chlorine microelectrodes unsuitable for routine measurements in the field. However, it is a reliable tool for fundamental studies of biocide mass transport phenomena in biofilms.

ACKNOWLEDGMENTS

We thank Ching-Tsan Huang and Xiao Chen for their help with the experiments and Anne Camper for suggesting the possibility of working with a chlorine electrode.

This work was supported by the Center for Biofilm Engineering at Montana State University, a National Science Foundation-sponsored Engineering Research Center (cooperative agreement EED-8907039), and by the Center's industrial associates.

REFERENCES

1. **American Public Health Association, American Water Works Association, and Water Environment Federation.** 1992. Standard methods for the examination of water and wastewater, 18th ed. American Public Health Association, Washington, D.C.
2. **Ben-Yaakov, S.** 1979. Halogen analysis by membrane covered polarographic sensors. J. Electroanal. Chem. **98**:15–24.
3. **Brown, M. R. W., and P. Gilbert.** 1993. Sensitivity of biofilms to antimicrobial agents. J. Appl. Bacteriol. Symp. Suppl. **74**:87–97.
4. **Camper, A. K.** 1993. Coliform regrowth and biofilm accumulation in drinking water systems: a review, p. 91–105. *In* G. G. Geesey, Z. Lewandowski, and H.-C. Flemming (ed.), Biofouling/biocorrosion in industrial systems. Lewis Publications, Inc., Chelsea, Mich.
5. **Characklis, W. G., and K. Marshall.** 1990. Biofilms: a basis for an interdisciplinary approach, p. 3–15. John Wiley & Sons, Inc., New York.
6. **Chen, C.-I., T. Griebe, and W. G. Characklis.** 1993. Biocide action of monochloramine on biofilm systems of *Pseudomonas aeruginosa*. Biofouling **7**:1–17.
7. **Costerton, J. W., K. J. Cheng, G. G. Geesey, T. I. Ladd, J. C. Nickel, M. Dasgupta, and T. J. Marrie.** 1987. Bacterial biofilms in nature and disease. Annu. Rev. Microbiol. **41**:435–464.
8. **de Beer, D., P. Stoodley, and Z. Lewandowski.** 1994. Liquid flow in heterogeneous biofilms. Biotechnol. Bioeng. **44**:636–641.
9. **de Beer, D., J. C. van den Heuvel, and S. P. P. Ottengraf.** 1993. Microelectrode measurements of the activity distribution in nitrifying bacterial aggregates. Appl. Environ. Microbiol. **59**:573–579.
10. **Ford, T., and R. Mitchell.** 1990. The ecology of microbial corrosion. Adv. Microb. Ecol. **11**:231–262.
11. **Griebe, T., C.-I. Chen, R. Srinivasan, and P. S. Stewart.** 1993. Analysis of biofilm disinfection by monochloramine and free chlorine, p. 151–161. *In* G. G. Geesey, Z. Lewandowski, and H.-C. Flemming (ed.), Biofouling/biocorrosion in industrial systems. Lewis Publications, Inc., Chelsea, Mich.
12. **LeChevallier, M. W., C. D. Cawton, and R. G. Lee.** 1988. Factors promoting survival of bacteria in chlorinated water supplies. Appl. Environ. Microbiol. **54**:649–654.
13. **LeChevallier, M. W., C. D. Lowry, and R. G. Lee.** 1988. Inactivation of biofilm bacteria. Appl. Environ. Microbiol. **54**:2492–2499.
14. **McCoy, W. F.** 1987. Effects of fouling biofilms on systems performance, p. 234–246. *In* M. W. Mittelman and G. G. Geesey (ed.), Biological fouling of industrial water systems: a problem solving approach. Water Micro Associates, San Diego, Calif.
15. **Nichols, W. W.** 1989. Susceptibility of biofilms to toxic compounds, p. 321–331. *In* W. G. Characklis and P. A. Wilderer (ed.), Structure and function of biofilms. John Wiley & Sons, Inc., New York.
16. **Perry, R. H., and C. H. Chilton.** 1973. Chemical engineers' handbook, 5th ed. McGraw-Hill, New York.
17. **Revsbech, N. P., and B. B. Jorgensen.** 1986. Microelectrodes: their use in microbial ecology. Adv. Microb. Ecol. **9**:293–352.
18. **van der Wende, E., W. G. Characklis, and D. B. Smith.** 1989. Biofilms and bacterial drinking water quality. Water Res. **23**:1313–1322.
19. **Yu, F. P., G. M. Callis, P. S. Stewart, T. Griebe, and G. A. McFeters.** Cryosectioning of biofilms for microscopic examination. Biofouling, in press.
20. **Yu, F. P., and G. A. McFeters.** 1994. Rapid in situ assessment of physiological activities in bacterial biofilms using fluorescent probes. J. Microbiol. Methods **20**:1–10.